Available online at www.sciencedirect.com
SCIENCE DIRECT
Journal of Molecular Structure 751 (2005) 85–94
Journal of MOLECULAR STRUCTURE
www.elsevier.com/locate/molstruc

Preparation, crystal structure and optical spectroscopy of the rare earth complexes (RE^{3+} = Sm, Eu, Gd and Tb) with 2-thiopheneacetate anion

Ercules E.S. Teotonio[a,*], Hermi F. Brito[a], Maria Cláudia F.C. Felinto[b], Larry C. Thompson[c], Victor G. Young[d], Oscar L. Malta[e]

[a]*Departamento de Química Fundamental, Instituto de Química da Universidade de São Paulo, 05508-900 São Paulo SP, Brazil*
[b]*Instituto de Pesquisas Energéticas e Nucleares Travessa R 400 Cidade Universitária, São Paulo-SP CEP 05508-970, Brazil*
[c]*Department of Chemistry, University of Minnesota, Duluth, MN 55812, USA*
[d]*Department of Chemistry, University of Minnesota, Minneapolis, MN 55455, USA*
[e]*Departamento de Química Fundamental CCEN, Universidade Federal de Pernambuco, Recife PE 50670-901, Brazil*

Received 18 March 2005; revised 29 April 2005; accepted 2 May 2005
Available online 27 June 2005

Abstract

Rare earth complexes with the formulae $Sm(TPAC)_3 \cdot 3H_2O$, $Eu_2(TPAC)_6 \cdot 5.25H_2O$ and $RE(TPAC)_3 \cdot 3.5H_2O$ (where RE = Gd and Tb), and TPAC = 2-thiopheneacetate) have been synthesized and characterized by complexometric titration, elemental analyses, infrared spectroscopy, and X-ray crystallography. Infrared data suggested the presence of both bridging and chelating TPAC anions. The crystal structure of the $[Eu_2(TPAC)_6 \cdot (H_2O)_3] \cdot 2.25H_2O$ complex in the solid state, determined by X-ray diffraction, revealed that it crystallizes in the orthorhombic crystal system (space group Aba2), with two crystallographically independent Eu^{3+} centers (Eu1 and Eu2). These europium centers are held together by one bidentate bridging and two tridentate bridging carboxylate groups. The existence of two Eu^{3+} centers was also supported by the emission spectrum. The luminescence properties of the RE–TPAC complexes were investigated by measuring the excitation and emission spectra, and the intramolecular ligand-to-rare earth energy transfer mechanisms were discussed. The emission spectra of the Eu^{3+} and Tb^{3+} ions displayed only narrow bands arising from $^5D_0 \rightarrow {}^7F_0$ and $^5D_0 \rightarrow {}^7F_{0-4}$ transitions, respectively, indicating an efficient luminescence sensitization of these ions by the TPAC 'antenna'. On the other hand, the emission spectrum of the Sm^{3+}-complex displayed a broad band from the phosphorescence of the TPAC ligand which overlapped the $4f^5$-intraconfigurational transitions. The theoretical intensity parameters Ω_λ ($\lambda = 2$ and 4), maximum splitting of the $^7F_1$ state (ΔE) and the ratio between the $^5D_0 \rightarrow {}^7F_0$ and $^5D_0 \rightarrow {}^7F_2$ transition intensities (R_{02}) were calculated based on the X-ray crystalline structure for the Eu^{3+}-complex, and a comparison with experimental data were made. The emission quantum efficiency (η) of the ^5D emitting level of the Eu^{3+} ion was also determined.
© 2005 Elsevier B.V. All rights reserved.

Keywords: Rare earths; 2-Thiopheneacetate; Crystalline structure; Intensity parameters; Intramolecular energy transfer

1. Introduction

Trivalent rare earth ions (RE^{3+}) are well known for their unique spectroscopic and magnetic properties which make them important in several technological, medical, and biological research areas. For example, the luminescence properties of RE^{3+}-compounds are used as optical signal amplifiers, emitting materials in electroluminescent devices, and fluoroimmunoassay probes in biological systems [1–4]. One of the most important properties of RE^{3+}-compounds is the very narrow absorption and emission bands arising from the parity-forbidden intraconfigurational 4f–4f transitions [2]. Consequently, the very weak absorption bands only have oscillator strengths around 10^{-6} and the photoluminescent spectra of the simple RE^{3+} ions in solution are also generally very weak when the excitation is in the ^{2S+1}L levels of the RE^{3+} ion. In order to overcome the effect of this low absorptivity, organic ligands with chromophoric groups are coordinated to the RE^{3+} ions and can act as 'antenna' [5], absorbing and transferring

* Tel.: +55 11 3091 3708; fax: +55 11 3815 5579.
E-mail address: ercules@iq.usp.br (E.E.S. Teotonio).

0022-2860/$ - see front matter © 2005 Elsevier B.V. All rights reserved.
doi:10.1016/j.molstruc.2005.05.001

energy efficiently to the rare earth ion and consequently increasing their luminescence quantum yield (q) [6].

The investigation of the luminescence properties of the Eu^{3+} and Tb^{3+} ions are of special relevance because of their strong red (~615 nm) and green (~545 nm) luminescences and also the long lifetimes of the excited $^5D_0$ and $^5D_4$ states, respectively. In particular, the special attention given to the Eu^{3+} ion is mainly due to the non-degenerate emitting level ($^5D_0$) which means that the emission bands arising from the $^5D_0 \rightarrow {}^7F_J$ transitions ($J=0$–4) can provide clearer information about the local symmetry [7]. On the other hand, the $^5D_4$ emitting level of the Tb^{3+} ion is ninefold degenerate which makes the assignment of the site symmetry from the emission spectrum a more difficult task. The Sm^{3+} ion is less studied due to its more complex energy level structure. However, some Sm-complexes exhibit intense orange luminescence arising from the intraconfigurational $^4G_{5/2} \rightarrow {}^6H_J$ transitions ($J=5/2$, 7/2, 9/2 and 11/2). The emitting $^4G_{5/2}$ level of the Sm^{3+} ion (~500 nm) is resonant with the triplet states (T) of many organic ligands and may offer an efficient energy transfer from ligand to rare earth ion ($T \rightarrow Sm^{3+}$) [8].

RE^{3+}-carboxylate complexes represent an important area within rare earth coordination chemistry both because the carboxylate group presents various coordination modes which lead to complex structures and because such compounds often display intense luminescence [9–11]. In particular, ligands containing five-membered heterocycles, such as the anions 2-thiophenecarboxylate (TPC), 2-thiopheneacetate (TPAC) and 2-furanecarboxylate (FUR), are excellent complexing agents, presenting three possible sites of coordination to metal ions [12–15], one from the S (TPC and TPAC) or O (FUR) of the heterocyclic group and two from the carboxylate group. However, owing to the hard acid behavior of the RE^{3+} ions, there is a strong affinity of these metal ions for hard base, negatively charged carboxylate oxygen donors. In most RE^{3+}-coordination compounds reported with TPC and FUR, the carboxylate groups are involved in the metal–ligand bonding by chelating and bridging coordination modes, forming dinuclear, polymeric or network structures.

The photophysical properties of RE^{3+}-complexes containing carboxylate anions have been extensively reported [10,16–19] and have been shown to act as luminescent sensitizers, especially for Eu^{3+} and Tb^{3+} ions, by an efficient intramolecular ligand-to-metal energy transfer. The triplet state (T) of TPAC around 25,000 cm^{-1} may act as an energy donor to the excited levels of Sm^{3+}, Eu^{3+} and Tb^{3+} ions (Fig. 1) [15].

This article reports the synthesis, characterization, crystal structure, and photoluminescence properties of the luminescent trivalent rare earth complexes (RE^{3+} = Sm, Eu, Gd and Tb) with TPAC. A detailed study of the photoluminescence properties of the RE-TPAC complexes was made in order to obtain information on the energy transfer process from the TPAC ligand to the RE^{3+} ions. Based on the crystal structure of the $[Eu_2(TPAC)_6\cdot(H_2O)_3]\cdot 2.25H_2O$ complex, the intensity parameters were calculated and compared with the experimental ones. In addition, the radiative and non-radiative rates and experimental emission quantum efficiencies were also investigated.

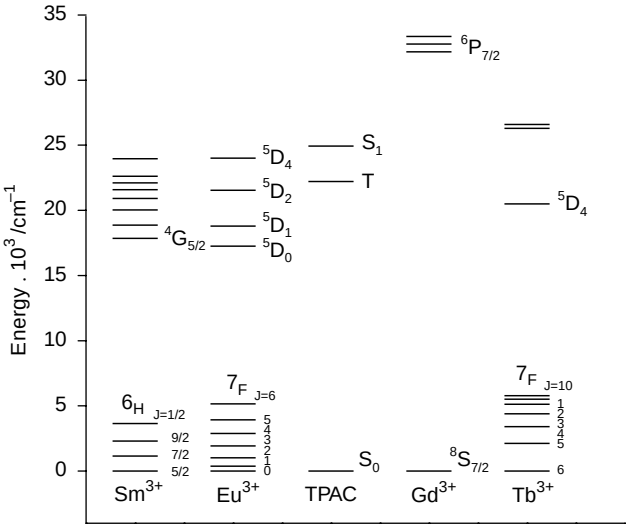


Fig. 1. Partial energy level diagram of the TPAC ligand states obtained from the phosphorescence spectrum of the Gd-complex, and some energy levels of the Sm^{3+}, Eu^{3+}, Gd^{3+} and Tb^{3+} ions.

2. Experimental

2-Thiopheneacetic acid (HTPAC) was purchased from Sigma-Aldrich and used without further purification. The $RECl_3\cdot 6H_2O$ (RE = Sm, Eu, Gd or Tb) was prepared by reaction between rare earth oxide and hydrochloric acid according to literature procedures [14].

2.1. Synthesis of the RE–TPAC complexes

For the synthesis of the RE^{3+}–TPAC complexes, 2-thiopheneacetic acid (1.0 g, 6.7×10^{-3} mol) was dissolved in water (~30 mL) and the anion was formed by addition of a solution of NaOH (1 mol L^{-1}) was added to pH ~ 7. An aqueous solution of $RECl_3\cdot 6H_2O$ (0.85 g, 2.34 mmol) was added dropwise to this solution and after 3 days colorless crystal were deposited. The crystal solid was filtered, washed with water and dried under vacuum to give the desired product (yields 80–90%).

2.2. Apparatus

Elemental analyses for carbon and hydrogen in the complexes were carried out on a Perkin–Elmer model 240 microanalyzer, while the RE^{3+} contents were determined by complexometric titration with EDTA. The infrared (IR) spectra were recorded in KBr pellets on a Bomen

model MB-102 spectrophotometer in the range of 400–4000 cm^{-1}.

X-ray crystallographic data were collected on an Enraf–Nonius CAD4 Mach3 single crystal diffractometer with graphite-monochromated Mo Kα radiation (λ = 0.71073 Å) at 298 K. The orientation matrix and cell dimensions were determined by least-squares refinement of the angular positions of 25 reflections. Data were processed on a Pentium PC and corrected for absorption and Lorentz polarization effects. The structure of the $[Eu_2(TPAC)_6 \cdot (H_2O)_3]$ complex was solved by the standard Patterson heavy atom method, followed by normal difference Fourier techniques. Space group, structure solution, refinement, molecular graphics and geometrical calculation have been carried out with the SHELX-L97 [20] and ZORTEP [21] programs. Owing to the low quality of the sample crystal all atoms except the Eu centers were refined isotropically.

The X-ray diffraction patterns were obtained on a Miniflex–Rigauku diffractometer using Cu Kα radiation (30 kV and 15 mA) in the interval of 4–70° (2) and 1 s of pass time, using the powder XRD method.

Steady-state luminescence measurements were performed with a spectrofluorometer (SPEX-Fluorolog 2) with a 0.22 m double grating monochromator (SPEX 1680), and a 450 W Xenon lamp as excitation source. To eliminate the second-order diffraction of the source radiation, a cut-off filter was used in the measurements. All excitation and emission spectra were recorded at room (~298 K) and liquid nitrogen (77 K) temperatures and collected at an angle of 22.5° (front face) using a detector mode correction. The luminescence decay curves of the emitting levels were measured using a phosphorimeter accessory (SPEX 1934D) coupled to the spectrofluorometer. The luminescence instruments were fully controlled by a DM3000F spectroscopic computer program and the spectral intensities were automatically corrected for the photomultiplier response.

3. Results and discussion

3.1. Characterization of the RE–TPAC complexes

The percentages of the rare earth ions (RE^{3+} = Sm, Eu, Gd and Tb), C and H are the following: Sm^{3+}-complex (Calcd: Sm, 23.94; C, 34,30; H, 3.37. Found: Sm, 23.80; C, 34.35; H, 4.05). Eu^{3+}-complex (Calcd: Eu, 24.40; C, 31.71; H, 3.26. Found: Eu, 24.51; C, 35.74; H, 3.40). Gd^{3+}-complex (Calcd: Gd, 24.35; C, 33.58; H, 3.91. Found: Gd, 24.42; C, 33.51; H, 3.10). Tb-complex (Calcd: Tb, 24.62; C, 33.49; H, 3.90. Found: Tb, 24.70; C, 33.53; H, 3.46). These results are consistent with the formulas $Sm(TPAC)_3 \cdot 3H_2O$, $Eu(TPAC)_3 \cdot 5.25H_2O$ and $RE(TPAC)_3 \cdot 3.5H_2O$ (RE = Gd and Tb).

The IR spectra of the RE-complexes (figure not shown) recorded from 400 to 4000 cm^{-1} are very similar, indicating similar coordination of the TPAC ligand to the RE ions. In order to investigate the coordination mode of the TPAC anion to the RE^{3+} ions, the infrared spectra of the complexes were compared to that of the sodium–TPAC salt [12]. The TPAC ligand in ionic form presents strong bands around 1428 and 1573 cm^{-1}, which are attributed to the $\nu_s(C=O)$ and $\nu_{as}(C=O)$ stretching vibrational modes, respectively. In the case of the RE^{3+}-complexes it was observed that each of these bands is split into two peaks, the first at 1392 and 1434 cm^{-1} and the second one at 1549 and 1602 cm^{-1}. These complexes present the separations of the asymmetric and symmetric stretching vibrations ($\Delta\nu_{(C=O)} = \nu_{as} - \nu_s$) around 210 and 115 cm^{-1}, which are in good agreement with the existence of a carboxylate group coordinated to the RE^{3+} ion by bidentate bridging and chelate forms [22]. The IR spectra also have a broad band around 3423 cm^{-1} assigned to ν(O–H), suggesting the presence of water molecules in these complexes.

3.2. Structural data for the europium complex

Single crystals of the Eu–TPAC complex were grown from the mother solution at room temperature (~298 K) over a period of 3 days. No sign of deterioration during storage under ordinary laboratory atmospheric conditions was observed. Crystallographic data for the structure determination of the Eu-complex are listed in Table 1. X-ray data reveal that this complex is isostructural with those RE^{3+}–TPAC-complexes (RE^{3+} = Ce, Pr, Nd and

Table 1
Crystal data and structure refinement for the $[Eu_2(TPAC)_6 \cdot (H_2O)_3] \cdot 2.25H_2O$ complex

Empirical formula	$C_{36}H_{38}Eu_2O_{16}S_6$
Formula weight	1222.94
Temperature K	2932
Wavelength (Å)	0.71073
Crystal system, space group	Orthorhombic, Aba2
Unit cell dimensions	
a (Å)	15.7462
b (Å)	19.8613
c (Å)	29.6804
$\alpha(°) = \beta(°) = \gamma(°)$	90.0
V (Å^3)	9198 2
Z	8
D_c (g cm^{-3})	1.766
Absorption coefficient (mm^{-1})	3.040
$F(000)$	4832
Limiting indices	$0 \le h \le 18$
	$0 \le k \le 23$
	$-35 \le l \le 33$
Reflections collected/unique	8061/5710 [Rint = 0.2187]
Refinement method	Full-matrix least-squares on F^2
Data/restraints/parameters	5710/0/201
Goodness-of-fit on F^2	1.212
Final R indices [$I > 2I$]	$R1 = 0.0633$
	$wR2 = 0.1457$
R indices all data	$R1 = 0.0652$
	$wR2 = 0.1465$

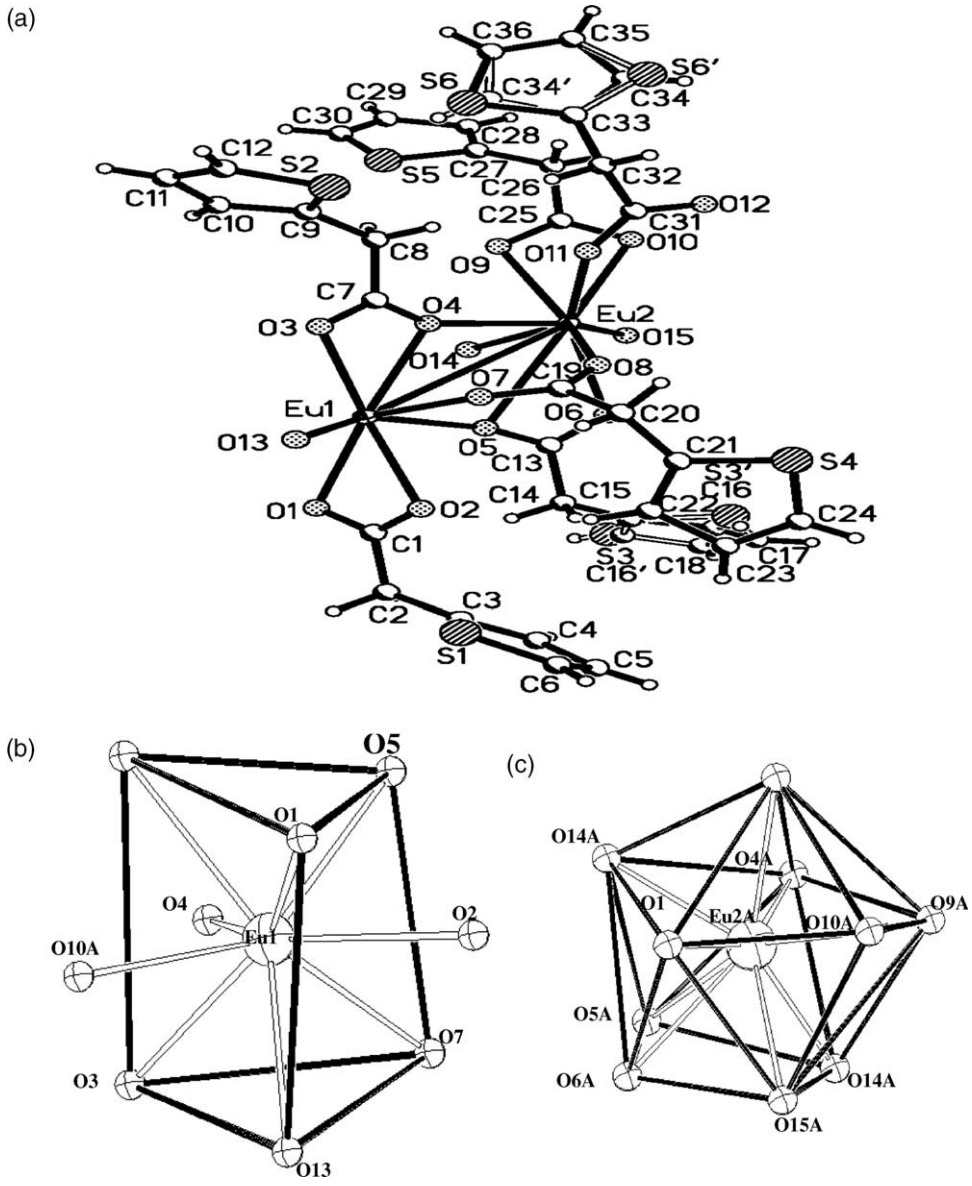


Fig. 2. Crystal structure of the $[Eu_2(TPAC)_6 \cdot (H_2O)_3] \cdot 2.25H_2O$ complex: (a) asymmetric unit; (b) distorted polyhedral coordination around the Eu1 center and (c) distorted polyhedral coordination around the Eu2A center.

Sm) recently reported by Cai and co-workers [15], which belong to the Aba2 space group in the orthorhombic system.

According to the single crystal X-ray analysis the Eu–TPAC-complex consists of asymmetric units forming infinite chains parallel to the *a*-axis. The unit cell contains two independent crystallographic sites for Eu ions, labeled Eu(1) and Eu(2A), each coordinated to three TPAC ligands. The molecular structure of the Eu-complex is shown in Fig. 2(a). The TPAC ligand is coordinated to the Eu(1) and Eu(2A) centers in the following coordination mode: bidentate chelating, bidentate bridging and chelating tridentate bridging, corroborating the IR data. It is interesting to note that the Eu2A center is deca-coordinated with two oxygen atoms from water molecules and eight from the TPAC ligand, while the Eu(1) center is nine-coordinated with only one oxygen atom from a water molecule and eight oxygen atoms from the TPAC ligand. As shown in Fig. 2(b), the coordination polyhedron of Eu(1) is a distorted tricapped trigonal prism, while the coordination geometry at the Eu(2A) can be described as a distorted bicapped dodecahedron (Fig. 2(c)). However, if the interaction O(5A)–Eu(2A) is not considered, due to its longer distance, the geometry at Eu(2A) can be also described as distorted tricapped trigonal prismatic.

The distances and angles from Eu(1) and Eu(2A) to the oxygen atoms in the first coordination spheres are listed in Table 2. The shortest europium–oxygen distances are 2.299 and 2.383 Å, corresponding to the interatomic distances Eu(1)–O(5) and Eu(2A)–O(8A), respectively.

Table 2
Bond lengths (Å) and selected angles (°) around the two crystallographically independent Eu^{3+} ions in the $[Eu_2(TPAC)_6\cdot(H_2O)_3]\cdot 2.25H_2O$ complex

Bond lengths (Eu1)			Bond lengths (Eu2A)		
Eu1–O1	2.512 (7)		Eu2A–O1	2.436 (7)	
Eu1–O2	2.506 (8)		Eu2A–O4A	2.425 (6)	
Eu1–O3	2.451 (7)		Eu2A–O5A	2.985 (11)	
Eu1–O4	2.589 (7)		Eu2A–O6A	2.517 (8)	
Eu1–O5	2.299 (7)		Eu2A–O8A	2.383 (7)	
Eu1–O7	2.370 (8)		Eu2A–O9A	2.491 (7)	
Eu1–O13	2.457 (9)		Eu2A–O10A	2.654 (8)	
Eu1–O10A	2.444 (6)		Eu2A–O11A	2.433 (6)	
Eu1–O12A	2.378 (7)		Eu2A–O14A	2.478 (10)	
			Eu2A–O15A	2.494 (11)	
Bond angles (Eu1)					
O1–Eu1–O2	51.3 (16)	O7–Eu1–O3	78.3 (3)	O10A–Eu1–O4	113.7 (2)
O1–Eu1–O3	145.5 (3)	O7–Eu1–O4	71.4 (3)	O10A–Eu1–O5	140.8 (3)
O2–Eu1–O3	142.8 (3)	O7–Eu1–O5	77.3 (4)	O10A–Eu1–O7	141.9 (3)
O4–Eu1–O1	151.0 (2)	O13–Eu1–O1	85.7 (3)	O10A–Eu1–O13	66.1 (3)
O4-Eu1-O2	137.(6)	O13-Eu1-O2	71.9 (5)	O12A-Eu1-O1	79.5 (2)
O4–Eu1–O3	51.1 (15)	O13–Eu1–O3	77.0 (3)	O12A–Eu1–O2	122.1 (3)
O5–Eu1–O1	89.1 (3)	O13–Eu1–O4	122.7 (3)	O12A–Eu1–O3	94.9 (3)
O5–Eu1–O2	76.5 (4)	O13–Eu1–O5	143.2 (4)0	O12A–Eu1–O4	74.5 (2)
O5–Eu1–O3	122.3 (3)	O13–Eu1–O7	76.7 (3)	O12A–Eu1–O5	73.9 (4)
O5–Eu1–O4	71.6 (3)	O10A–Eu1–O1	68.3 (2)	O12A–Eu1–O7	140.7 (2)
O7–Eu1–O1	126.3 (3)	O10A–Eu1–O2	108.7 (3)	O12A–Eu1–O13	140.0 (3)
O7–Eu1–O2	75.0 (3)	O10A–Eu1–O3	77.6 (3)	O12A–Eu1–qO10A	70.9 (3)
Bond angles (Eu2A)					
O1–Eu2A–O4A	153.2 (3)	O10A–Eu2A–O1	66.2 (2)	O14A–Eu2A–O5A	62.2 (4)
O5A–Eu2A–O1	118.7 (2)	O10–Eu2A–O4A	121.4 (2)	O14A–Eu2A–O6A	74.7 (3)
O5A–Eu2A–O4A	63.1 (18)	O10A–Eu2A–O5A	162.0 (3)	O14A–Eu2A–O8A	127.7 (3)
O6A–Eu2A–O1	79.0 (2)	O10A–Eu2A–O6A	125.6 (3)	O14A–Eu2A–O9A	69.9 (3)
O6A–Eu2A–O4A	108.6 (2)	O10A–Eu2A–O8A	130.6 (3)	O14A–Eu2A–O10A	101.6 (3)
O6A–Eu2A–O5A	45.6 (17)	O10A–Eu2A–O9A	49.9 (15)	O14A–Eu2A–O11A	138.2(3)
O8A–Eu1–O1	78.5 (3)	O11A–Eu2A–O1	79.5 (2)	O15A–Eu2A–O1	70.0 (4)
O8A–Eu1–O4A	78.7 (3)	O11A–Eu2A–O4A	80.5 (2)	O15A–Eu2A–O4A	136.7 (4)
O8A–Eu1–O5A	66.3 (3)	O11A–Eu2A–O5A	128.9 (3)	O15A–Eu2A–O5A	99.5 (3)
O8A–Eu1–O6A	76.3 (4)	O11A–Eu2A–O6A	145.1 (3)	O15A–Eu2A–O6A	64.4 (4)
O9A–Eu2A–O1	115.9 (2)	O11A–Eu2A–O8A	72.6 (3)	O15A–Eu2A–O8A	133.1 (4)
O9A–Eu2A–O4A	74.8 (2)	O11A–Eu2A–O9A	73.7 (3)	O15A–Eu2A–O9A	86.1(4)
O9A–Eu2A–O5A	123.6 (2)	O11A–Eu2A–O10A	68.1 (2)	O15A–Eu2A–O1OA	64.9 (3)
O9A–Eu2A–O6A	140.9 (4)	O14A–Eu2A–O1	135.2 (3)	O15A–Eu2A–O11A	131.1 (3)
O9A–Eu2A–O8A	139.8 (3)	O14A–Eu2A–O4A	70.9 (3)	O15A–Eu2A–O14A	66.1 (4)

It is important to note that the oxygen atoms from each chelate carboxylate group of TPAC are coordinated differently to the Eu^{3+} ions, presenting a stronger and a weaker Eu–O interaction. These data are different from those for the Eu–TPC complex reported in Ref. [13], in which the distances between the Eu and O atoms are similar.

The distances Eu(1)–Eu(2) and Eu(1)–Eu(2A) in the $[Eu_2(TPAC)_6\cdot(H_2O)_3]\cdot 2.25H_2O$ complex are equal to 4.2609 and 4.1592 Å, respectively. Although, these distances are similar to those reported for the $[RE_2(TPAC)_6\cdot(H_2O)_3]$ compounds (RE = Ce, Pr and Sm) [15], it is observed that there is a trend in these distances: they decrease as the atomic number increases.

X-ray powder diffraction patterns (Figure not shown) of the RE^{3+}–TPAC compounds were obtained from 4 to 70° and are very similar, indicating the presence of isomorphism for this series of compounds.

3.3. Photoluminescence investigation

3.3.1. Phosphorescence of the Gd^{3+}–TPAC complex

The photophysical properties of the TPAC donor states in the rare earth complexes were examined based on the phosphorescence spectrum of the Gd–TPAC complex. Since there is a large energy gap ($\sim$32,000 cm^{-1}) between the $^8S_{7/2}$ ground state and first $^6P_{7/2}$ excited state of the Gd^{3+} ion, it cannot accept any energy from the first excited triplet state of the TPAC via intramolecular ligand-to-metal energy transfer (Fig 3).

In contrast to the $La^{3+}(4f^0)$ and $Lu^{3+}(4f^{14})$ ions that are, respectively, larger and smaller than the Eu^{3+} ion, the Gd^{3+} ion is very similar in size to Eu^{3+}. Consequently, the effect of these latter rare earth ions on the TPAC ligand states should also be similar [23].

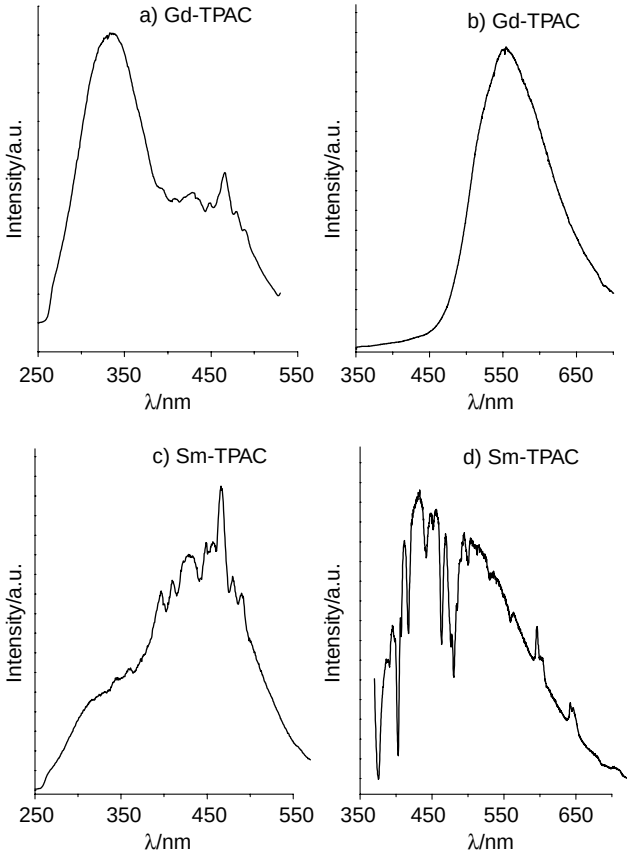


Fig. 3. Luminescence spectra of the Gd^{3+}-complex: (a) excitation and (b) emission. Luminescence spectra of the Sm^{3+}-complex: (c) excitation and (d) emission.

The excitation spectrum of the $Gd(TPAC)_3 \cdot 3.5H_2O$ complex recorded in the spectral range from 250 to 500 nm, at 77 K, is shown in Fig. 3(a).

This spectrum exhibits a broad band with a maximum around 330 nm which may be attributed to the ligand-centered $S_0 \rightarrow S_1$ (π,π^*)transition of the thiophene moiety. The emission spectrum of the Gd-complex (Fig 3b) in the spectral range 420–700 nm displays a broad band with a maximum around 550 nm when excited in the $S_0 \rightarrow S_1$ transition ($\sim$330 nm). The luminescence decay curve of this transition was recorded and the higher value of the emitting state lifetime ($\tau = 4.87$ ms) provides evidence about the triplet state character of this state, indicating that this band may be assigned to the TPAC phosphorescence due to the $T \rightarrow S_0$ transition.

From the phosphorescence band the energy of the triplet state (T) was determined as the shortest wavelength 0–0 transition around 450 nm. It is interesting to observe that the energy of the T state is above the energies of the main emitting levels, $^4G_{5/2}$ (Sm^{3+}), ($^5D_0$) Eu^3, and ($^5D_4$) Tb^{3+}(Fig. 1), indicating that the TPAC ligand can act as an antenna to photosensitize the rare earth ions, collecting UV energy and transferring it in a non-radiative process through the T state to the resonant excited state of these rare earth ions [3].

3.3.2. Luminescence of the Sm^{3+}–TPAC complex

In spite of the possibility of energy transfer from the TPAC ligand to the Sm^{3+} ion, the $Sm(TPAC)_3 \cdot 3.5H_2O$ complex displays only a very weak orange luminescence when excited with UV radiation. As can be seen in Fig 3c, the excitation spectrum of the Sm^{3+}-complex recorded in the spectral range 250–590 nm, at 77 K, shows a broad and intense band between 300 and 420 nm with a maximum around 330 nm, which is attributed to the ligand-centered TPAC transition. Furthermore, an important feature of the excitation spectrum of the Sm^{3+} complex is the presence of several intense narrow bands arising from the $4f^5$-intraconfigurational-transitions from the $H_{5/2}$ ground state to the following excited levels (nm): $^4H_{9/2}$ (345), $^4F_{9/2}$ (363), $^4L_{17/2}$ (375), $^4H_{11/2}$ (390), $^4F_{7/2}$ (403), $^4M_{19/2}$ (417), $^4I_{15/2}$ (442), $^4F_{3/2}(1)$ (452), ^4I (463), $^4I_{11/2}$ (478), $^4G_{7/2}$ (499), $^4F_{3/2}(2)$ (530) and $^4G_{5/2}$ (560). These narrow bands overlap the broad band from the TPAC ligand.

The emission spectrum of the Sm^{3+}–TPAC complex recorded from 420 to 720 nm with excitation at 330 nm (Fig. 3(d)) consists of a broad phosphorescence band from the TPAC ligand. These data indicate that the TPAC ligand keeps its emission when excited at shorter wavelengths. According to these results there is no efficient intramolecular energy transfer from TPAC to the Sm^{3+} ion. An important feature in the emission spectrum of the Sm^{3+} complex is the presence of some 'dips' inside the phosphorescence broad band that are attributed to the absorption lines corresponding to the following transitions (nm): $^6H_{5/2} \rightarrow {}^4H_{9/2}$ (345), $^4F_{9/2}$ (363), $^4L_{17/2}$ (375), $^4H_{11/2}$ (390), $^4F_{7/2}$ (403), $^4M_{19/2}$ (417), $^4I_{13/2}$ (463) and $^4I_{11/2}$ (478).

The narrow emission bands assigned to the $^4G_{5/2} \rightarrow {}^6H_J$ transitions ($J = 5/2$, 7/2, 9/2 and 11/2) of the Sm ion exhibit low intensities and overlap the stronger phosphorescence band from the TPAC ligand. This is in contrast to the spectrum of the Sm^{3+}–TPC complex reported in Ref. [13] where the hypersensitive $^4G_{5/2} \rightarrow {}^6H_{9/2}$ transition was dominant.

3.3.3. Luminescence of the Eu^{3+}–TPAC complex

Fig. 4(a) shows, the steady-state excitation spectrum of the $[Eu_2(TPAC)_6 \cdot (H_2O)_3] \cdot 2.25H_2O$ complex recorded in the spectral range from 250 to 590 nm, with emission monitored on the hypersensitive $^5D_0 \rightarrow {}^7F_2$ transition at 612 nm. This spectrum consists of narrow bands assigned to the $4f^6$-intraconfigurational transitions from $^7F_0$ to the excited states (nm): $^5G_6$ (361), $^5H_4$ (374), $^5L_6$ (394), $^5D_2$ (464), $^5D_1$ (532) and $^5D_0$ (578), and a broad band centered around 330 nm, which is attributed to the $S_0 \rightarrow S_1$ transition of the TPAC ligand. This latter band indicates that the Eu^{3+} ion is clearly sensitized by the 2-thiophene chromophore. It should be mentioned that the excitation band from the ligand is almost as intense as the narrow band arising from the $^7F_0 \rightarrow {}^5L_6$ transition ($\sim$394 nm), indicating that the Eu^{3+}–TPAC compound presents similar bright luminescence via direct and indirect excitation.

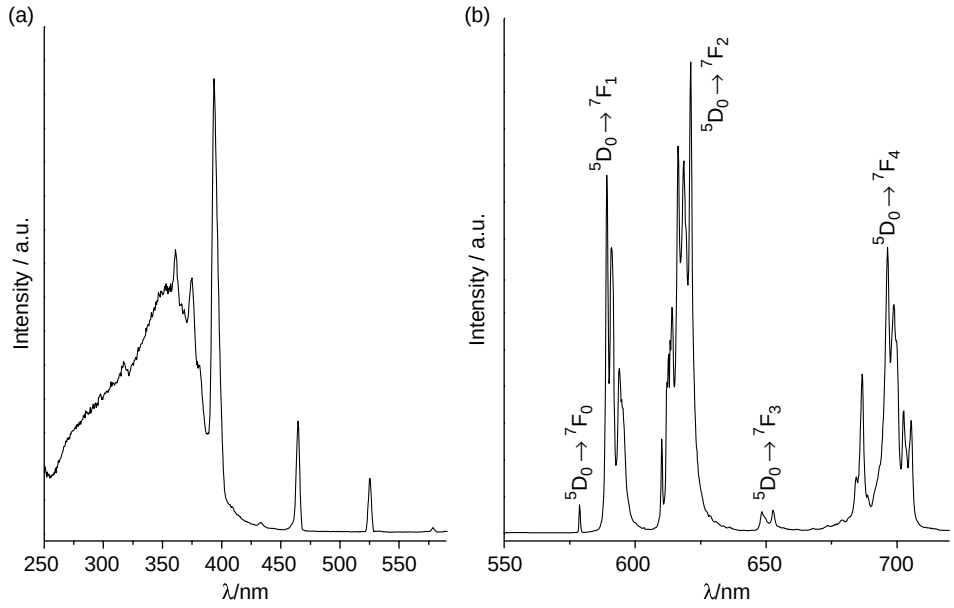


Fig. 4. Luminescence spectra of the $[Eu_2(TPAC)_6 \cdot (H_2O)_3] \cdot 2.25H_2O$ complex in solid state, at 77 K: (a) excitation spectrum with emission monitored in the hypersensitive $^5D_0 \rightarrow {}^7F_2$ transition of the Eu^{3+} ion at 612 nm and (b) emission spectrum monitored on the TPAC ligand band, at 320 nm.

The emission spectrum of the Eu–TPAC-complex recorded in the range from 420 to 720 nm under excitation at 394 nm ($^7F_0 \rightarrow {}^5L_6$ transition), at 77 K, is presented in Fig. 4(b). As shown in this figure the emission spectrum of the Eu–TPAC-complex exhibits intense narrow bands corresponding to the $^5D_0 \rightarrow {}^7F_J$ transitions ($J=0$–4). Furthermore, no phosphorescence broad band from the ligand has been observed in this spectrum, indicating that the triplet state of the TPAC plays an important role in the luminescence sensitization of the Eu^{3+} ion.

A detailed analysis of the emission spectrum of the Eu–TPAC-complex (Fig. 4(b))reveals the existence of more than $(2J+1)$-components for the $^5D_0 \rightarrow {}^7F_J$ transitions. For example, the $^5D_0 \rightarrow {}^7F_0$ transition is observed to be asymmetric with a maximum at 17,277 cm^{-1} with a shoulder around 16,949 cm^{-1}. According to these data, in the Eu–TPAC compound there are two different Eu centers having different chemical environments with site symmetries of the type C_s, C_n or C_{nv}. This is in agreement with the X-ray crystal structure of the Eu–TPAC complex, which shows that the geometry of the oxygen atoms coordinated to (Eu1) is close to C_{3v} symmetry. It is also observed that the splitting of the $^5D_0 \rightarrow {}^7F_0$ transition is small for the Eu ions in these two crystallographic centers, suggesting that the ligand fields at these centers are not markedly different. This is consistent with the X-ray crystal structure, which shows that if the longest distance, Eu2A–O(5), is neglected, the two Eu(1) and Eu(2A) sites have similar structures.

The luminescence decay curve of the $^5D_0$ emitting level of the Eu-complex recorded under excitation at 394 nm and emission at 612 nm reinforces the existence of two Eu centers, since the profile of this curve fits very well to a bi-exponential law. In this context, the emission quantum efficiency (η) of the $^5D_0$ emitting level, radiative (A_{rad}) and

Table 3
Spherical coordinates of the oxygen atoms bonded to the Eu^{3+} sites (Eu1 and Eu2A) in the $[Eu_2(TPAC)_6 \cdot (H_2O)_3] \cdot 2.25H_2O$ compound

Eu-TPAC	Eu1 site			Eu2A site		
	R (Å)	θ	ϕ	R (Å)	θ	ϕ
TPAC oxygen	2.512	60.00	16.52	2.436	55.18	5.84
	2.505	18.35	319.98	2.986	63.51	7.17
	2.450	146.42	48.13	2.518	31.21	320.42
	2.589	121.11	342.73	2.383	55.67	85.47
	2.299	58.63	305.76	2.491	163.43	67.54
	2.370	68.84	33.43	2.653	118.11	27.41
	2.444	124.53	352.72	2.434	114.68	310.08
	2.378	115.33	76.16	2.477	105.95	320.34
H_2O oxygen	2.457	87.70	290.09	2.425	119.73	37.04
				2.493	77.65	79.90

Table 4
Experimental and theoretical 4f-4f intensity parameters, charge factors and polarizabilities (optimum values) for some complexes

Complexes	$\Delta E_{exp.}$	$\Delta E_{teor.}$	$R_{02(exp.)}$	$R_{02(teor.)}$	$\Omega_{2(exp.)}$	$\Omega_{2(teor.)}$	Ω_2^{ed}	Ω_2^{dc}	$\Omega_{4(exp.)}$	$\Omega_{4(teor.)}$	Ω_4^{ed}	Ω_4^{dc}	g(L)	$g(H_2O)$	α(L)	$\alpha(H_2O)$
$[Eu(TTA)_3(H_2O)_2]$	205	202	0.0130	0.0120	33.0	19.8	0.1	18.5	4.6	4.7	0.30	7.1	1.0	2.0	4.0	1.0
$[Eu(TPC)_3(H_2O)_2]$	90	119	0.0037	0.0024	15.8	16.9	0.5	18.3	8.2	6.4	0.06	7.3	0.5	0.6	2.0	4.4
$[Eu_2(TPAC)_6\cdot(H_2O)_3]\cdot 2.25H_2O$																
Eu1 site	193	199	0.0034	0.0037	4.7	5.7	0.6	6.0	7.7	3.2	0.05	3.9	1.1	1.1	2.2	3.1
Eu2A site	193	193	0.0034	0.0036	4.7	5.9	1.5	5.4	7.7	3.4	0.13	4.5	1.3	1.3	2.4	1.7

radiationless (A_{nrad}) rates, and experimental intensity parameters (Ω_2 and Ω_4) for the Eu–TPAC-complex were determined as an average value containing the contribution of both Eu1 and Eu2A centers.

The emission quantum efficiency (η) of the $^5D_0$ emitting level in $[Eu_2(TPAC)_6\cdot(H_2O)_3]\cdot 2.25H_2O$ at room temperature was obtained based on the luminescence data (emission spectrum and emission decay curve of this compound recorded at ~298 K). Eq. (1) provides a means to determine the η value from experimental spectroscopic data [3].

$$\eta = \frac{A_{rad}}{A_{rad} + A_{nrad}} \tag{1}$$

where the coefficients A_{rad} represent the radiative contribution of the forced electric dipole $^5D_0 \rightarrow {}^7F_2(A_{02})$ and $^5D \rightarrow {}^7F(A_{04})$ transitions. The magnetic dipole $^5D_0 \rightarrow {}^7F_1$ transition (A_{01}) was used as internal standard owing to its almost insensitive behavior to the chemical environment around the Eu^{3+} ion. The denominator in Eq. (1) is calculated from the lifetime of the emitting level ($1/\tau = A_{rad}+A_{nrad}$). The values of radiative (A_{rad}), radiationless (A_{nrad}) rates and lifetime of the emitting $^5D_0$ level are 304, 807 s^{-1} and 0.899 ms, respectively.

The value of η determined for the $[Eu_2(TPAC)_6\cdot(H_2O)_3]\cdot 2.25H_2O$ complex is low (~27.4%) due to the high frequency O–H vibrations of the water molecules in the first coordination sphere of the rare-earth ion which deactivate the excited Eu^{3+} ion level, efficiently quenching its luminescence. Such behavior is in agreement with the higher value of the non-radiative rate ($A_{nrad} = 807\ s^{-1}$). The value of η for the $[Eu_2(TPAC)_6\cdot(H_2O)_3]\cdot 2.25H_2O$ complex is larger than for the Eu–TPC-compound [13]. These results show that the presence of only three water molecules coordinated to the Eu^{3+} emitting centers (one at Eu1 and two at Eu2A) provide a less effective non-radiative de-excitation pathway in the TPAC complex, in contrast to the binuclear Eu–TPC, where two water molecules are coordinated to each Eu^{3+} ion, resulting in a non-radiative rate ~2376 s^{-1}.

The experimental intensity parameters (Ω_2 and Ω_4) for the Eu–TPAC-complex were determined using Eq.(2), following the method reported in Ref. [3]

$$\Omega_\lambda = \frac{4e^2\omega^3 A_{0\lambda}}{3\hbar c^3 \chi \langle {}^7F \| U^{(\lambda)} \| {}^5D_0 \rangle^2} \tag{2}$$

where $A_{0\lambda}$ are the coefficients of spontaneous emission for the $^5D_0 \rightarrow {}^7F_\lambda$ transitions ($\lambda = 2$ and 4), χ is the Lorentz local field correction term that is given by $\chi = n(n^2+2)^2/9$, with the refractive index $n = 1.5$, and $\langle {}^7F \| U^{(\lambda)} \| {}^5D_0 \rangle^2$ are the squared reduced matrix elements whose values are 0.0032 and 0.0023 for $\lambda = 2$ and 4, respectively. The theoretical intensity parameters Ω_λ were obtained according to the theory of 4f–4f intensities [3]. These parameters depend on both the chemical environment and the rare earth ion,

and are given by the equation

$$\Omega_\lambda = (2\lambda + 1)\sum_{t,p}\frac{|B_{\lambda tp}|^2}{(2t+1)} \quad (3)$$

where the quantities $B_{\lambda tp}$ are known as the intensity parameters of individual transitions between Stark levels, containing both forced electric dipole (ED) and dynamic coupling (DC) contributions [3].

In order to investigate, the nature of the chemical environment around the rare earth ion, the intensity parameters Ω_λ were calculated using the coordination geometry (in spherical coordinates) obtained from the DRX structure (Table 3). The isotropic polarizability (α_j) and the charge factor (g_j) of the jth donor atom, at position $\longrightarrow R_j$ were treated as freely varying parameters within ranges of physically acceptable values by assuming two types of oxygen donor atoms (carboxylate and water oxygen atoms). In the theoretical study, the ligand field parameters were given by the simple overlap model (SOM) [3]. The same values of experimental intensity parameters (Ω_2 and Ω_4), R_{02} and ΔE, for both Eu1 and Eu2A centers were used (Table 4). The values of these parameters together with the values obtained for g(TPAC), g(H_2O), α(TPAC) and α(H_2O) are presented in Table 4. The experimental value of Ω_2 4.7×10^{-20} cm^2 is low as compared to those for Eu-β-diketonate and Eu–TPC complexes, revealing a low degree of covalent bonding (Eu^{3+}–O) in the TPAC-complex. Table 4 also gives the contributions to the forced electric dipole mechanism ($\Omega_\lambda^{e.d}$, $\alpha_j=0$) and dynamic coupling mechanism ($\Omega_\lambda^{d.c}$, $g_j=0$) for each Eu center. The values of $\Omega_2^{d.c}=18.3$ and $\Omega_4^{d.c}=7.3$ are higher than $\Omega_2^{e.d}=0.48$ and $\Omega_4^{e.d}=0.06$ (in units of 10^{-20} cm^2), suggesting that the dynamic coupling is by far the dominant mechanism to the radiative transitions in the Eu^{3+}–TPAC-complex. Since in this mechanism the intensity of the hypersensitive transitions is related explicitly to the polarizabilities of the ligands, a comparison of the $\Omega_2^{d.c}$ value for Eu–TPAC with the one for Eu–TPC [24] gives evidence of a moderate polarizable chemical environment around the Eu^{3+} centers in the complex containing the TPAC ligand (Table 4).

3.3.4. Luminescence of the Tb^{3+}–TPAC complex

The excitation spectrum (Fig 5a) of the $Tb(TPAC)_3\cdot3.5H_2O$ complex recorded at 77 K monitoring the $^5D_4\rightarrow{}^7F_5$ transition (542 nm) consists of a broad band in the range from 250 to 330 nm, attributed to the ligand centered singlet–singlet transition. In addition to this band, narrow bands arising from 4f–4f transitions from the ground state $^7F_5$ level (nm) to the $^5L_6$ (339), $^5L_9$ (350), $^5L_{10}$ (369), $^5G_6$ (376), $^5D_3$ (380) and $^5D_4$ (488) excited levels are observed. It is very interesting that the relative intensity of the broad band is higher than those from the rare earth ion, indicating that the indirect excitation processes is more operative in the Tb–TPAC complex.

Fig. 5(b) shows the emission spectrum of $Tb(TPAC)_3\cdot3.5H_2O$ at 77 K recorded from 420 to 720 nm, with photoexcitation at 330 nm. This spectrum shows only the expected sequence of narrow bands assigned to the $^5D_4\rightarrow{}^7F_{0-6}$ transitions from the terbium ion, which is dominated by the sensitive $^5D_4\rightarrow{}^7F_5$ transition around 545 nm. The absence of the broad band due to the phosphorescence of TPAC indicates an efficient intramolecular energy transfer (TPAC–Tb^{3+}).

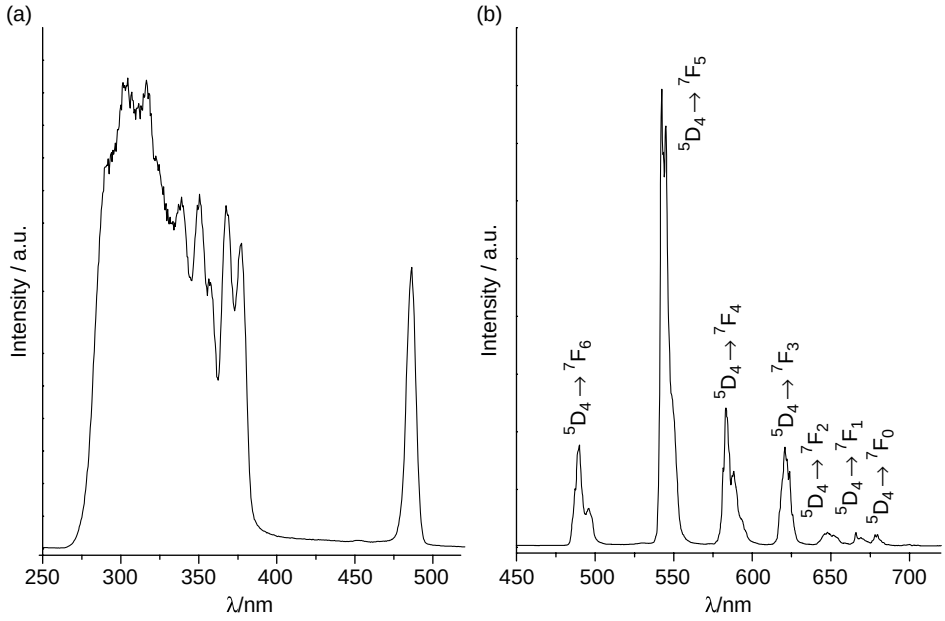


Fig. 5. Luminescence spectra of the $Tb(TPAC)_3\cdot3.5H_2O$ complex in solid state, at 77 K: (a) excitation spectrum under emission on the hypersensitive $^5D_4\rightarrow{}^7F_5$ transition of the Tb^{3+} ion, at 542 nm and (b) emission spectrum monitored on the TPAC ligand band, at 330 nm.

4. Conclusions

Synthesis, characterization, and a photoluminescence study of the RE-TPAC complexes (RE = Sm^{3+}, Eu^{3+}, Gd^{3+}, Tb^{3+}) demonstrate that the TPAC ligand is coordinated to the metal ion by chelating bidentate and bidentate- and tridentate-bridging through carboxylate oxygen atoms. Single crystal structural data for the Eu-TPAC complex demonstrated that there are two crystallographic europium ions. However, the luminescence data suggested that the ligand fields at these centers are not markedly different. In spite of the larger distance from the thiophene moiety to the Eu ion an efficient energy transfer from the $T_1(\pi,\pi^*)$ state to this ion was observed, which resulted in intense red emission. The same behavior was observed for the Tb^{3+}-complex, which showed an intense green luminescence arising from the $^5D_4 \rightarrow {}^7F_{0-6}$ transitions. In contrast, the Sm-complex displayed a broad band from the TPAC ligand that overlapped the $^4G_{5/2} \rightarrow {}^6H_j$ transitions, indicating an inoperative intramolecular energy transfer.

The theoretical values of the intensity parameters (Ω_λ, R_{02}) calculated from the structural data of the $[Eu_2(TPAC)_6 \cdot (H_2O)_3] \cdot 2.25H_2O$ complex are in good agreement with the experimental values. The values of these parameters were compared with those for the TPC and diketonate complexes, suggesting that the europium ion is in a moderately polarizable chemical environment.

Acknowledgements

This research was supported by grants from the Fundação de Amparo à Pesquisa do Estado de São Paulo (FAPESP) and the Conselho Nacional de Desenvolvimento Científico e Tecnológico (CNPq-RENAMI).

References

[1] I.A. Hemmilä, Application of Fluorescence in Immunoassays, Wiley, New York, 1991.
[2] J.-C.G. Bünzli, G.R. Choppin (Eds.), Lanthanide Probes in Life, Chemical and Earth Sciences—Theory and Practice, Elsevier, Amsterdam, 1989.
[3] G.F. de Sá, O.L. Malta, C.M. Donegá, A.M. Simas, R.L. Longo, P.A. Santa-Cruz, F. da Silva Jr., Coord. Chem. Rev. 196 (2000) 165.
[4] R. Reyes, M. Cremona, E.E.S. Teotonio, H.F. Brito, O.L. Malta, Chem. Phys. Lett. 396 (2004) 54.
[5] N. Sabatini, M. Guardigli, J.M. Lehn, Coord. Chem. Rev. 123 (1993) 201.
[6] G.E. Buono-Core, H. Li, Coord. Chem. Rev. 99 (1990) 55.
[7] F.S. Richardson, Chem. Rev. 82 (1982) 541.
[8] H.F. Brito, O.L. Malta, M.C.F.C. Felinto, E.E.S. Teotonio, J.F.S. Menezes, C.F.B. Silva, C.S. Tomiyama, C.A.A. Carvalho, J. Alloys Comp. 344 (2002) 293.
[9] F.A. Hart, in: G. Wilkinson, R.D. Gillard, J.A. McCleverty (Eds.), Comprehensive Coordination Chemistry vol. 3, Pergamon, Oxford, 1987 Chapter 38.
[10] B. Barja, R. Baggio, M.T. Garland, P.F. Aramendia, O. Pena, M. Perec, Inorg. Chim. Acta 346 (2003) 187.
[11] B. Yan, Q.Y. Xie, J. Mol. Struct. 688 (2004) 73.
[12] X. Li, K. Jin, S. Lu, J. Zhang, J. Mol. Struct. 604 (2002) 65.
[13] L. Yuan, Z. Li, J. Sun, K. Zhang, Spectroch. Acta 59 (2003) 2949.
[14] E.E.S. Teotonio, M.C.F.C. Felinto, H.F. Brito, O.L. Malta, A.C. Trindade, R. Najjar, W. Strek, Inorg. Chim. Acta 357 (2004) 451.
[15] L.Z. Cai, W.T. Chen, M.S. Wang, G.C. Guo, J.S. Huang, Inorg. Chem. Commun. 7 (2004) 611.
[16] L. Yuan, Z. Li, J. Sun, K. Zhang, Spectroc. Lett. 32 (1999) 867.
[17] P.P. Barthelemy, G.R. Choppin, Inorg. Chem. 28 (1989) 3354.
[18] Z.M. Wang, L.J. van de Burgt, G.R. Choppin, Inorg. Chim. Acta 310 (2000) 248.
[19] P.R. Selvin, J. Jancarik, M. Li, L.W. Hung, Inorg. Chem 35 (1996) 700.
[20] G.M. Sheldrick, SHELX-97, Program for Crystal Structure Solution, Göttingen University, Germany, 1997.
[21] G.M. Sheldrick, SHELX-97, Program for Crystal Structure Solution, Göttingen University, Germany, 1997.
[22] G.B. Deacon, R.J. Phillips, Coord. Chem. Rev. 33 (1980) 251.
[23] R.D. Archer, H. Chen, L.C. Thompson, Inorg. Chem. 37 (1998) 2089.
[24] H.F. Brito, O.L. Malta, M.C.F.C. Felinto, E.E.S. Teotonio, J.F.S. Menezes, C.F.B. Silva, C.S. Tomiyama, C.A.A. Carvalho, J. Alloys Comp. 344 (2002) 293.